JJBS

Volume 17, Number 1,March 2024
ISSN 1995-6673
Pages 89 – 98
https://doi.org/10.54319/jjbs/170108

Jordan Journal of Biological Sciences

Novel Thiazolidinedione Linked 1,3,4-Oxadiazole Derivatives as AXL Inhibitors Targeting Breast Cancer: *In-Silico* Design, ADMET Screening, and MM-GBSA Binding Free Energy

Mahendra Gowdru Srinivasa[1], Ananya Dinesh Rao[1], Ancilla Laveena Dsouza[1], Gauthami R[1], Jackson Loy Monteiro[1], Shridhar Deshpande N[1], Natasha Naval Aggarwa1[1], Banylla Felicity Dkha rGatphoh[1], Revanasiddappa B.C[1]

[1]*Department of Pharmaceutical Chemistry, NGSM Institute of Pharmaceutical Sciences (NGSMIPS), Nitte (Deemed to be University), Mangalore-575018, (Karnataka) India ;*

Received: May 4, 2023; Revised: July 17, 2023; Accepted: July 20, 2023

Abstract

A new series of thiazolidinedione linked 1,3,4oxadiazole hybrid analogs (T1-25) were designed by In-silico approach for their AXL inhibitor activity against breast cancer. Molecular docking studies were performed with binding pocket of AXLinhibitor (PDB ID: 5TD2) by using Schrodinger suit 2020- to elucidate the binding interactions of the newly designed targets. The docking studies were performed for all the designed molecules by Prime-MMGBSA module to determine free energy, In-silico ADMET screening by QikProp and Glide module. Based on the Glide score, the binding affinity of all the designed molecules towards AXL was chosen. AXL was inhibited by the designed molecules that have good hydrogen bonding interactions. The molecules (T1-25) have significant Glide scores in the range of -3.847 to -9.181 when compared with the standard Cyclophosphamide (-3.847) and 5-fluorouracil (-6.233). The In-silico molecular docking, ADMET properties were found within the suggested values. The MM-GBSA binding free energy results displayed very promising activity with the selected AXL inhibitor. The compounds T15, T19, T21 and T22 with highest Glide scores were found to be significant for anti-breast cancer activity.

Keywords: 2,4-thiazolidinone, 1,3,4-oxadiazoles, In-silico analysis, MM-GBSA, AXL inhibitor, Breast cancer.

1. Introduction

In the United States, breast cancer is the second most common cancer among women and the second largest cause of cancer death (Musetti et al.,2021; Savitri et al., 2023). Malignancies are including lung, breast, prostate, gastric, ovarian, and thyroid, have high levels of AXLkinase (Ito et al.,1999). Hepatocellular leukemia and acute myeloid leukemia have also been shown to be over expressed (Heet al., 2021). In 2020, 2,79,100 new cases are expected to be diagnosed in the United States, with over 42,000 deaths due to this kind of cancer (Siegel et al.,2016). Cancer molecular targeted therapy has become a research priority in recent years. Tyrosine kinase inhibitors (TKIs) that are targeting the platelet-derived growth factor receptor (PDGFR), vascular endothelial growth factor (VEGF), and epidermal growth factor receptor (EGFR),(Jänne et al.,2015)have shown promise in clinical studies, prompting researchers to investigate for additional diagnostic and prognostic markers (Subbiah et al.,2017;Gay et al.,2017).

In chronic myeloid leukemia (CML) sufferers, the AXL gene on chromosome 19q13.2 was found (Feneyrolles et al., 2014). The Greek term "anexelekto" means "uncontrollable." The AXL gene produces the protein AXL (UFO, ARK, Tyro7, or JTK11). Compared to normal tissues, the level of AXL expression in cancer tissues is higher (Narukawa et al.,2020). By activating AXL kinase, several signaling pathways involved in cell proliferation, metastasis (Paccez et al., 2015), and apoptosis inhibition (Gjerdrum et al 2010; Nazreen et al.,2014) are activated. Due to its strong correlation with tumour growth, metastasis, inadequate survival, and drug resistance, AXL has become a desirable target for cancer therapy. AXL signalling supports the immunosuppressive and pro-tumorigenic phenotypes in the tumour microenvironment where it is expressed in cellular components. Preclinical investigations have shown that a range of AXL inhibitors are effective.

Insulin sensitizers known as thiazolidinediones (glitazones) are used to treat type 2 diabetes. They are having high-affinity towards Peroxisome proliferator-activated receptor (PPARc) ligands that reduce insulin resistance and effectively lower plasma glucose levels (Chen et al., 2015; Hu et al 2020). Thiazolidinedione derivatives have also been found to be anti-inflammatory, antibacterial, and anticancer drugs (Shankar et al.,2020; Tokala et al.,2018). Compounds that activate PPAR-c have been suggested to induce cancer cell differentiation (Trotsko et al.,2018). For example, the TZD analogue efatutazone (CS-7017) is a strong PPAR-c agonist and cancer differentiation inducer (Shimazaki et al., 2008). By inhibiting the insulin growth factor 1 (IGF1) pathway's constituent parts and changing the activity of the AMP-activated protein kinase (AMPK) pathway, PPAR-c

agonists have been proven to reduce cancer risk (Smallridge et al.,2013; Belfiore et al.,2009). Thiazolidinedione derivatives have anticancer effects through various mechanisms, including Blockade of the PI3K/Aktand Raf/MEK/ERK signaling pathways by inhibiting PI3K-a (Lee et al.,2008).

The wide range of applications for 1,3,4-oxadiazoles, on the other hand, renders them an interesting potential in medicinal chemistry. The pharmacophore 1,3,4-oxadiazole derivative has a potential antineoplastic impact in the treatment of several malignancies (Knight et al.,2010; Liu et al.,2012). Recently, new 1,3,4-oxadiazole containing thiazolidinedione derivatives have been identified as possible AXLinhibitors(Shen et al.,2019).Combining substantial bioactive pharmacophores into a complex measure is critical in medicinal chemistry for producing physiologically active molecules with distinct properties(Xu et al.,2020). To our knowledge, no studies on the anticancer effects of thiazolidinedione derivatives as AXL inhibitors have been reported. To discover possible AXL inhibitors, we tried to combine thiazolidinedione and 1,3,4- oxadiazole under one design. In silico analysis of AXL inhibitory actions were described in this paper. All the designed molecules were subjected to docking investigations in order to better understand the molecular mechanisms interactions (Alzhrani et al.,2020).

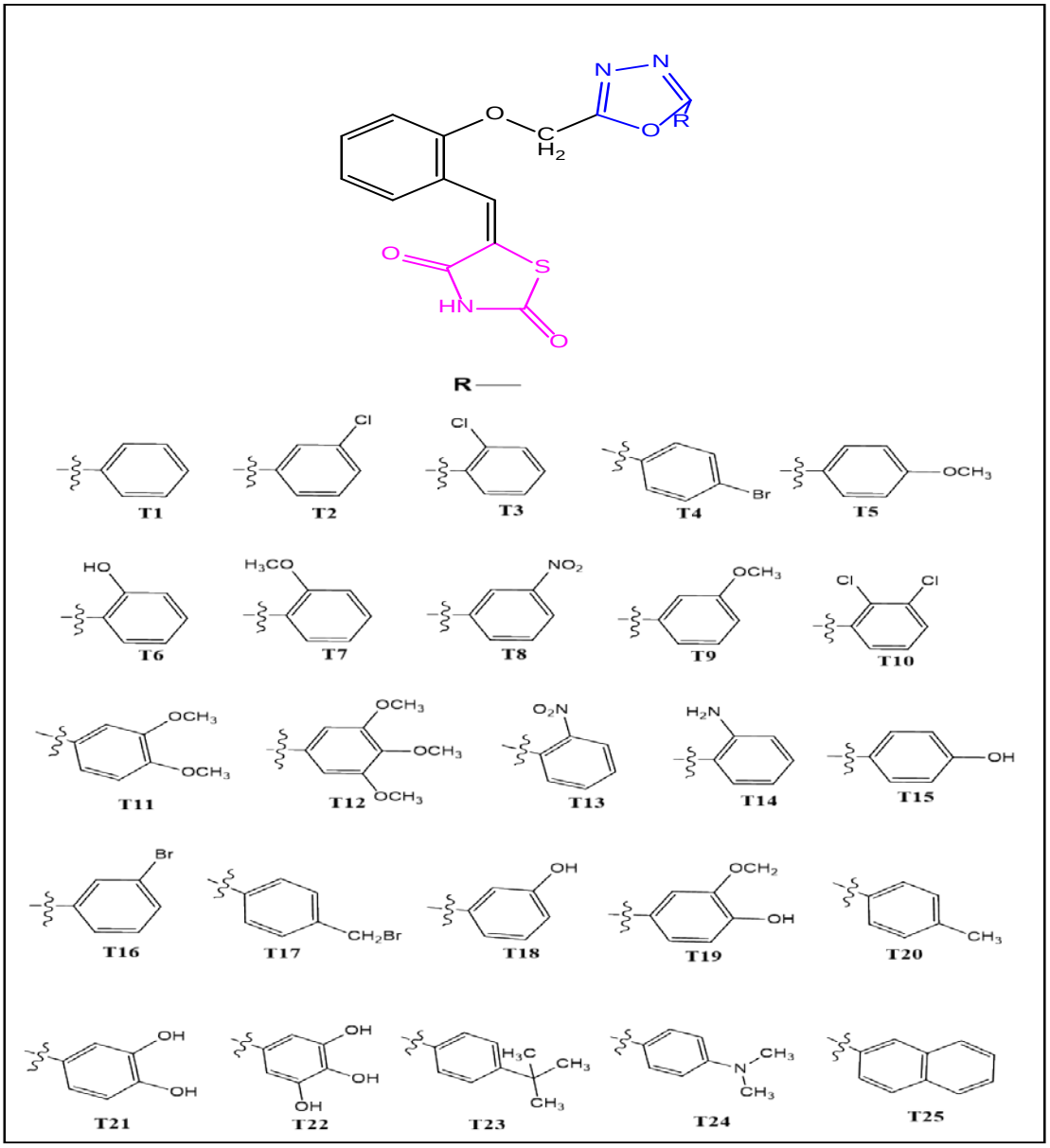

Figure 1. Design of Thiazolidinedione linked 1,3,4-oxadiazole molecules (T1-T25)

2. Materials and Methods

2.1. Molecular Docking

In-silico computer simulations were used to better understand the binding manner of the designed molecules with the target. The binding properties of the molecules were carried out with the Maestro 11.4 of Schrodinger suite 2020-3version (Batra et.al., 2021).

2.2. Ligand Preparation

A new series of designed thiazolidinedione linked 1,3,4 oxadiazole molecules(T1-T25) were constructed by using chemdraw software (figure-1). The chemical library was converted from 2D to 3D formats; geometry optimisation, bond order selection, and ligand ionisation state creation (through Epik) were done using the Ligprep module of the Schrodinger suite-2020-3. The OPLS-3E forcefield was utilized to reduce the energy of the ligands' 3D structures. Optimized ligands were further taken for docking studies. The docking structures should be a good representation of actual ligand structures as they appear in a protein-ligand complex to get better docking scores. Because the docking tools will only change the ligand's torsional coordinates, the reset of the geometric patterns should be optimized first, implying that the structures placed into the docking system should match all required standard conditions. The ligands that had been optimized to fit all the criteria were then used for docking experiments.

2.3. Protein Preparation

The protein data bank was used to obtain crystal structures with precise PDB IDs. Protein Preparation Wizard was used to optimize the chain. Assigning bond order, adding hydrogens, and handling disulfide are all part of the protein's preprocessing. Water molecules that were 5 Å distant from the hetero groups were eliminated entirely. The remaining water molecules' orientation was corrected, and hydrogen bonding was allocated. A and B chains were found in the crystal structure of 5TD2 with a resolution of 2.68Å. Chain A was favored because it was complete, with no missing residues.

Chain A was taken up for further studies to achieve a better binding approach. The preferred chains of the crystal structures were pre-processed using Schrodinger 2020-3 module. Generation of Het states was done using Epik at pH 7. Refinement of the protein was carried out by optimization by using PROPK, including sample water orientation. Waters with less than 3 H-bonds to non-waters were removed. OPLS-3E reduced the protein's size. Finally, the energy of the protein structure was decreased to energy Root Mean Square Deviation (RMSD) 0.30 Å utilizing the OPLS-3E force field. This is important to avoid steric conflicts by reorienting the hydroxyl groups in the side chains. The docking of the ligand against the protein was done in the first pocket of the protein molecule. The Figure 2 showed phi and phi scattering of amino acid residues, which were visualized by plotting the protein using the Ramachandran method.

2.4. Receptor grid generation

The 5TD2 crystal structures have been picked. The default parameters of the Receptor grid generation tool were utilized for grid generation by the Schrodinger 2020-3 suite. The ligand was contained within the box that encloses the centroid. The grid created could help the ligands in the same manner as the conventional derivatives.

2.5. Docking

Generation of conformers and orientation in the binding pocket take place in the presence of grid potentials (Al-Khayyat et. al., 2021). To exclude the ligand poses which do not correspond to a well-docked result, Hierarchical filters are used. The extra precision (XP) model was used to conduct a flexible ligand docking study of the designed compounds by the OPLS-3E force field. The ligands were prepared, and a specific grid was used for the analysis. Confirmations for every ligand were generated automatically by the docking process. Hierarchical filters are applied to the obtained ligand poses to estimate the ligand-receptor interaction. A penalty for the state of Epik was added to the docking score. Docking was used to expose ligands. To soften the potential of non-polar parts of the ligand, the partial charge cut-off was kept at 0.15 and the Van der Waal radii of the ligand atoms were scaled to 0.8. For all dockings, the default settings of the Glide module were kept. The co-crystallized ligand was first removed from the generated protein and redocked at the binding site to check the RMSD and other properties of the docking programme. To compare the docked and reference conformations, the RMSD value is employed. RMSD value will be less (Ideally less than 1 Å) when redocking or cross-docking is performed. RMSD is primarily used to verify the method used for docking studies. In molecular docking, RMSD was calculated to compare the docked conformation of the reference ligand with the original conformation of the reference ligand and validate the protein-bound ligand, which is docked in the same pocket check the deviation. The RMSD values were 0.1293Å for 5TD2. These were the most negligible RMSD value and are selected for further studies. At the ligand-binding site, all of the proposed ligands were docked with the protein. The dock score results from XP docking were summarized and studied.

2.6. MM-GBSA Assay

It is a post-docking experiment for determining the relative binding affinity of ligands that stands for Molecular mechanics with generalized Born and surface area solvation. A lower number indicates a stronger binding because the MM-GBSA binding energies are near to binding free energies. Prime MM-GBSA refines binding energy calculations using the VSGB solvation model, which uses the variable dielectric generalized Born model, water as a solvent, and the OPLS-3E force field. The docked molecules were selected, and Prime MM-GBSA binding free energy calculations were performed with respect to the desired minimized protein. After XP docking, the protein complexes and the designed ligands were further taken for energy calculations. The minimized protein was included, the desired ligands with better docking scores were selected, and the MM-GBSA job was run using the Prime MM-GBSA tool. This module aims to facilitate calculations of ligand binding energies and ligand strain energies, using prime technology.

2.7. ADMET studies

All the designed molecules were subjected for ADMET descriptors approach by using Schrodinger's Suite and Qikprop toxicity prediction procedure, and the ADMETSAR dataset (freely available at http://www.admetexp.org) was employed.

3. Results and Discussion

3.1. Molecular docking studies

Molecular Docking of the designed molecules (T1-T25) was performed in the groove of the target binding site, which played an essential role as a signal transducer in breast cancer and targeted to AXL receptor (Dey et al.,2021). In terms of G score, the binding affinity of all the derivatives is shown in Table-1. It is found that the binding free energy of all these derivatives ranged from -9.181 to -3.847 kcal/mol. Compounds T22, T21, and T19 are having the most refined binding energies with a binding score of -9.181, -8.503, and -7.556, respectively (Fig-2, 3, and 4). Compound T22 showed the highest binding affinity towards a target with binding free energies of -9.181. In compound T22, hydrogen bonding interactions of hydroxyl and carbonyl group substitution on the thiazolidinedione and phenyl ring were observed with Leu593 and Glu595, respectively. The interaction is observed in Figure-2. The other interactions with the amino acids are Gly594, Gly596, Val601, Ala617, Lys619, Met650, Leu671, Pro672, Phe673, Met674, Lys675, Gly677, Asp678, Asp728, Met730, Ala740, and Asp741 were observed. In compound T21, carbonyl and hydroxyl groups have hydrogen bond interaction and are observed with Leu593 and Glu595, respectively (Figure -3). Val601, Ala617, Met650, Leu671, Pro672, Phe673, Met674, Lys675, Gly677, Asp678, Asp728, Met730, Ala740, and Asp741 interaction were observed. In compound T19, hydrogen bonding interactions of carbonyl group substitution on the Thiazolidinedione ring were observed with Glu595. Gly594, Gly596, Val601, Ala617, Lys619, Met650, Leu671, Pro672, Phe673, Met674, Lys675, Gly677, Asp678, Asp728, Met730, Ala740, and Asp741.

In standard compound Methotrexate, hydrogen bonding interactions of nitro group in the ring structure are observed with amino acid Met674, the salt bridge was observed with carboxyl group with Lys591. (Figure-5). The other interactions with the amino acids are Lys591, Leu593, Gly594, Val601, Glu603, Asn605, Lys615, Ala617, Met650, Pro672, Phe673, Met674, Lys675, Tyr676, Gly677 and Met730 were observed. Based on the docking scores, the selected candidates were found to be suitable for AXL receptor activity.

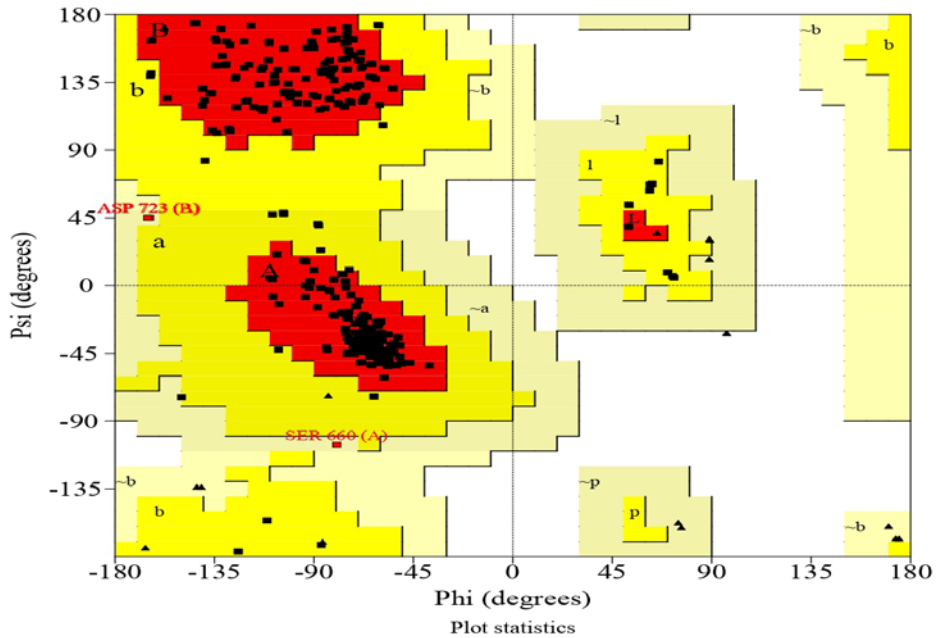

Figure-2: Ramachandran plot

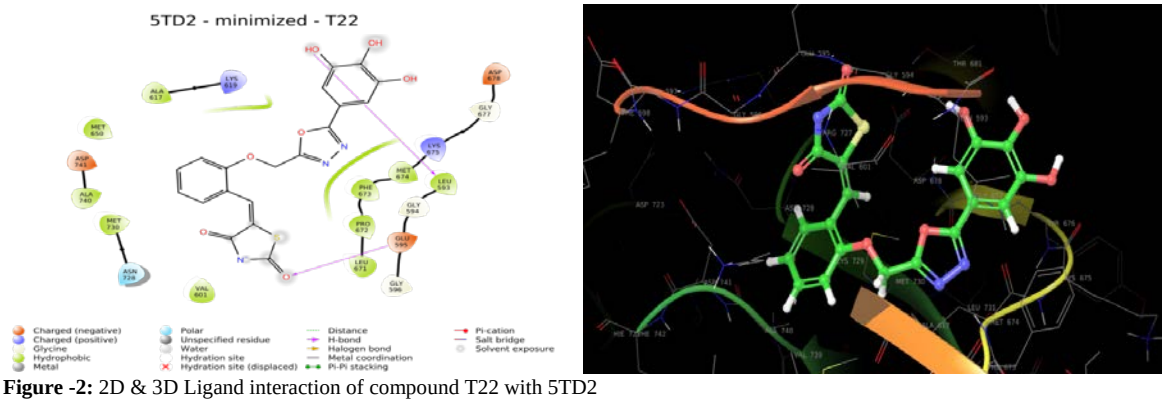

Figure -2: 2D & 3D Ligand interaction of compound T22 with 5TD2

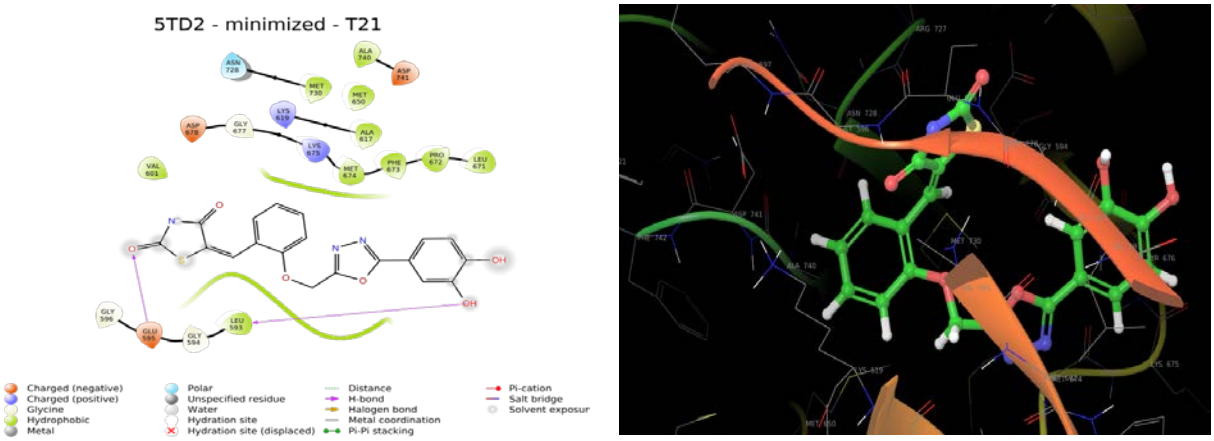

Figure-3: 2D & 3D Ligand interaction of compound T21 with 5TD2

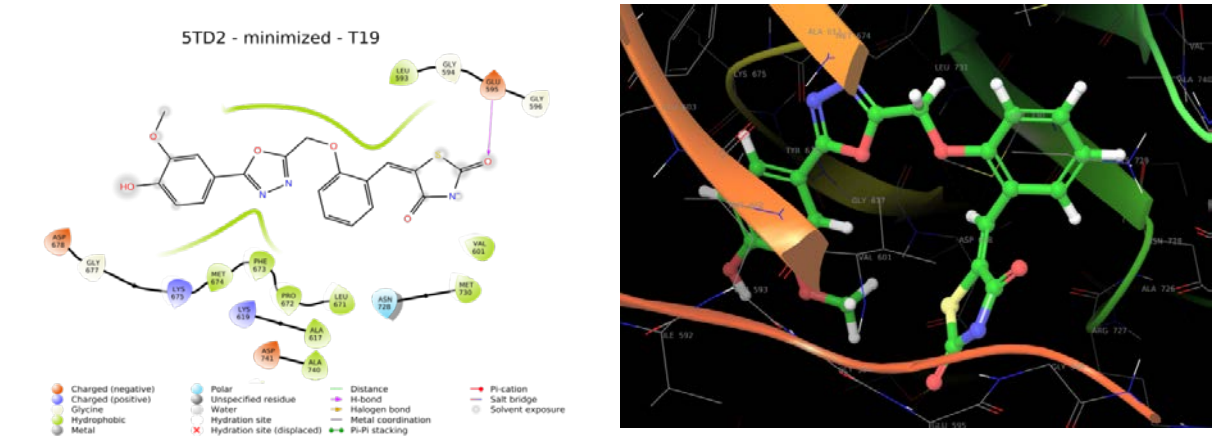

Figure 4: 2D & 3D Ligand interaction of compound T19 with 5TD2

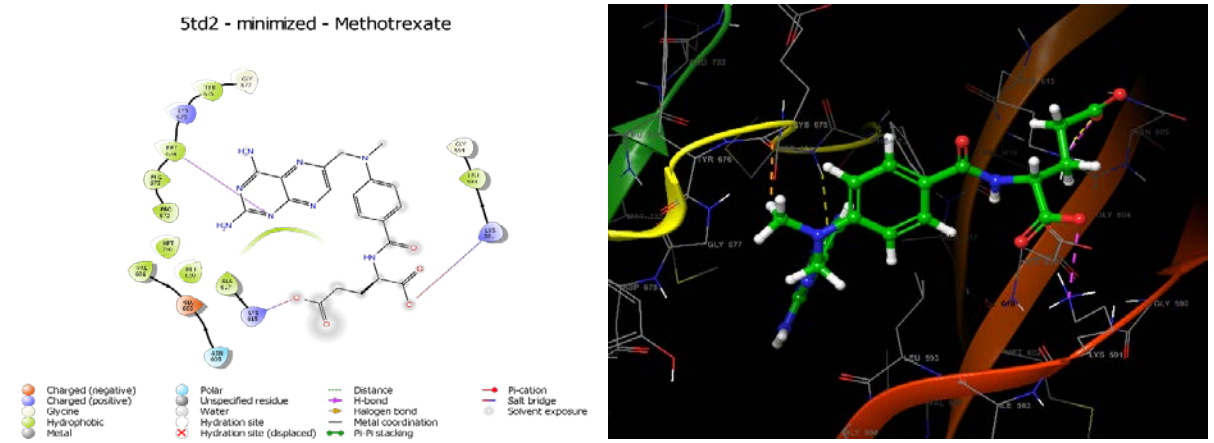

Figure -5: 2D & 3D Ligand interaction of compound Methotrexate with 5TD2

Table 1: Docking studies for compounds (T1-T25) with AXL inhibitor (5TD2)

Compounds	Glide score	Glide EvdW	XP H Bond	Glide emodel	G Rotab bonds	Glide ecoul
T1	-5.448	-42.524	0	-62.614	5	-4.192
T2	-6.945	-44.396	-1.032	-73.108	5	-6.354
T3	-6.29	-43.454	-0.172	-68.057	5	-6.681
T4	-5.505	-44.702	-0.198	-62.813	5	-8.932
T5	-6.942	-43.732	-1.084	-73.359	6	-9.132
T6	-6.621	-45.067	-0.742	-77.338	5	-3.284
T7	-5.61	-45.486	-0.199	-69.048	6	-7.367
T8	-6.115	-46.142	-0.399	-71.168	6	-5.988
T9	-6.2	-43.071	-0.51	-65.386	6	-6.023
T10	-6.727	-46.7	-0.938	-76.418	5	-7.493
T11	-6.057	-43.882	-0.203	-67.537	7	-5.96
T12	-6.267	-47.765	-0.302	-67.522	8	-5.044
T13	-6.028	-43.699	-0.358	-68.888	5	-6.211
T14	-6.187	-41.55	-0.199	-66.333	5	-6.804
T15	-7.004*	-43.728	-1.038	-74.21	6	-6.113
T16	-6.996	-45.167	-1.033	-77.154	5	-5.696
T17	-5.702	-42.606	-0.424	-65.653	6	-6.884
T18	-6.117	-42.077	-0.47	-66.217	6	-6.121
T19	-7.556*	-45.815	-1.512	-76.106	7	-6.372
T20	-6.054	-40.812	-0.208	-63.784	5	-6.616
T21	-8.503*	-43.252	-2.002	-76.886	7	-13.021
T22	-9.181*	-40.463	-2.076	-81.517	8	-18.769
T23	-6.528	-45.972	-0.625	-76.683	6	-5.918
T24	-6.025	-42.294	-0.41	-66.144	6	-6.593
T25	-6.729	-46.827	-0.35	-81.337	5	-6.661
Methotrexate (Std)	-8.485	-43.149	-1.212	-60.083	10	-4.359
5-fluorouracil (Std)	-6.233	-14.544	-1.086	-27.3	0	-2.36
Cyclophosphamid (Std)	-3.847	-21.907	0	-29.144	5	-5.692

Glide score: glide score; Glide EvdW: glide van der Waals energy; XP H Bond: extra precision hydrogen bonding;Glideemodel: glide model energy; G Rotatable bonds: Glide Rotatable bonds; Glide Ecoul: glide Coulomb energy

Table 2: Binding free energy calculation using Prime/MM-GBSA approach of compounds (T1-T25)

Comp	ΔG bind (Kcal/ mol)	ΔG bind Coulomb	ΔG bind covalent	ΔG bind Vander	ΔG bind H Bond	ΔG bind Lipophilic
T1	-79.88	-0.24	-0.83	-43.58	-0.71	-36.4
T2	-81.59	-0.05	-2.23	-39.81	-0.9	-42.54
T3	-79.32	-1.39	-2.87	-35.97	-0.94	-41.22
T4	-92.44	-21.33	-3.02	-45.23	-0.72	-41.57
T5	-92.46	-23.07	-2.27	-46.09	-0.93	-40.3
T6	-90.94	-21.97	-0.9	-46.82	-1.05	-39.41
T7	-90.72	-20.61	-0.73	-47.77	-0.9	-42.54
T8	-83.83	3.7	-0.64	-47.37	-0.72	-40.76
T9	-81.77	1.69	-2.12	-40.95	-0.71	-40.49
T10	-81.04	1.16	-2.94	-36.88	-0.71	-44.44
T11	-80.7	-1.02	3.09	-45.77	-0.72	-43.65
T12	-82.66	5.17	0.86	-44.91	-1.34	-40.25
T13	-79.43	0.25	0.69	-45.82	-1.13	-41.2
T14	-75.62	-1.6	-3.02	-36.5	-0.71	-39.69

T15	-79.8	-0.26	0.72	-40.69	-0.79	-41.47
T16	-82.16	-0.23	-2.17	-40.23	-0.72	-41.16
T17	-91.43	-21.7	-5.77	-45.97	-0.92	-38.14
T18	-81.25	-7.77	2.05	-42.42	-0.95	-40.62
T19	-79.07	-1.28	1.98	-44.19	-0.72	-42.71
T20	-78.46	0.89	-2.48	-39.83	-0.72	-39.72
T21	-92.51	-31.59	0.77	-43.85	-1.18	-39.36
T22	-75.14	9.58	2.61	-45.2	-3.42	-30.23
T23	-68.45	-4.02	-3.8	-33.71	-0.93	-38.94
T24	-81.73	2.37	-6.73	-44.25	-0.93	-39.57
T25	-81.48	-0.36	-2.39	-41.68	-0.93	-37.6
Methotrexate (Std)	-55.04	78.51	7.07	-51.06	-4.23	-30.59
5-fluorouracil (Std)	-21.78	-1.7	0.12	-17.34	-0.48	-7.36
Cyclophosphamid (Std)	-49.32	-8.82	6.31	-23.6	-0.8	-37

Δ G bind:free energy of binding; ΔG bind Coulomb:Coulomb energy; ΔG bind covalent: covalent energy (internal energy); ΔG bind Vander:van der Waals energy; ΔG bind H Bond:hydrogen bonding energy; ΔG bindLipophilic:hydrophobic energy (non-polar contribution estimated by solvent accessible surface area).

Table 3: Compliance of active thiazolidinedione linked 1,3,4oxadiazole derivatives (T1-T25) to electronic parameters of drug likeness and toxicity

Compounds	ADME descriptors and their probabilities											
	BBB+	HIA+	$Caco_2$	CYP	CYPIP	HERGI	Non AMES toxicity	Non carcinogens	Fish toxicity	Aqueous solubility (LogS)	Caco-2 permeability	Rat acute toxicity
T1	0.8186	1.000	0.6024	0.5430	0.5606	0.9778	0.5114	0.8268	0.8312	-3.3285	0.9878	2.3033
T2	0.8248	1.000	0.5893	0.5787	0.9203	0.9687	0.5687	0.7510	0.7756	-4.0323	1.0609	2.3299
T3	0.8248	1.000	0.5893	0.5787	0.9203	0.9687	0.5687	0.7510	0.7756	-4.0323	1.0609	2.3299
T4	0.8219	1.000	0.5939	0.6216	0.9395	0.9799	0.5660	0.7846	0.8299	-3.9035	1.0333	2.3730
T5	0.6151	1.000	0.5762	0.8638	0.8850	0.9744	0.5029	0.8491	0.8383	-3.1650	1.0702	2.3473
T6	0.5844	0.9965	0.6664	0.7039	0.6055	0.9850	0.5520	0.8143	0.9753	-3.1369	0.6442	2.2804
T7	0.6151	1.0000	0.5762	0.8638	0.8850	0.9744	0.9092	0.8491	0.8383	-3.1675	1.7072	2.3473
T8	0.6951	0.9947	0.5898	0.6649	0.9603	0.9277	0.7566	0.7588	1.0979	-3.6576	1.9017	2.4672
T9	0.6151	1.0000	0.5762	0.8638	0.8850	0.9744	0.5092	0.8491	0.8383	-3.1675	1.0702	2.3473
T10	0.8248	1.0000	0.5893	0.8665	0.9203	0.9687	0.5687	0.7510	0.7756	-4.0323	1.0609	2.3299
T11	0.5427	1.0000	0.5733	0.8466	0.8522	0.9809	0.5284	0.8300	0.8048	-3.2153	1.1021	2.3750
T12	0.5117	1.0000	0.5660	0.8456	0.8391	0.9793	0.5424	0.8116	0.7938	-3.3533	1.1938	2.3696
T13	0.7288	1.0000	0.6358	0.7590	0.7620	0.9857	0.5076	0.8072	0.9515	-3.3204	0.9443	2.2810
T14	0.7184	1.0000	0.5896	0.8756	0.9121	0.9746	0.5066	0.8122	0.8115	-3.3648	1.0635	2.2860
T15	0.5844	0.9956	0.6664	0.7039	0.6055	0.9850	0.5520	0.8143	0.9753	-3.1369	0.6442	2.2804
T16	0.8219	1.0000	0.5939	0.8475	0.9395	0.9799	0.5660	0.7876	0.8299	-3.9035	1.0333	2.3730
T17	0.7967	1.0000	0.5910	0.8240	0.9397	0.9787	0.5164	0.7846	0.8070	-3.5368	1.0638	2.4108
T18	0.5844	0.9956	0.6664	0.8589	0.6055	0.9850	0.5520	0.8143	0.9753	-3.1369	0.6442	2.2804
T19	0.8212	0.9953	0.6474	0.7533	0.6224	0.9827	0.5487	0.8411	0.9853	-3.0050	0.7298	2.3198
T20	0.7184	1.0000	0.5896	0.8756	0.9121	0.9746	0.5066	0.8122	0.8151	-3.3548	1.0635	2.2860
T21	0.7060	0.9891	0.6730	0.6340	0.5167	0.9840	0.5717	0.8260	0.9874	-3.0264	0.4770	2.3065
T22	0.7615	0.9774	0.6764	0.5969	0.5381	0.9845	0.5799	0.8394	1.0347	-2.9691	0.3577	2.3214
T23	0.5190	1.0000	0.5799	0.7389	0.8588	0.9935	0.5966	0.7418	0.6703	-3.8643	1.2083	2.4377
T24	0.5989	1.0000	0.5480	0.6371	0.6053	0.9696	0.5557	0.7435	0.7998	-3.3714	1.1102	2.4220
T25	0.8150	1.0000	0.6007	0.8328	0.8918	0.9741	0.5088	0.8402	0.7561	-3.7114	0.9726	2.3191

Table 5: Calculation of electronic parameters of drug likeness or oral bioavailability of the thiazolidinedione linked 1,3,4oxadiazole derivatives (T1-T25) by using Qikprop

Compounds	Mol. MW	HB donor	HB acceptor	QPPCaco	QPlogBB	QPPMDCK	Percent human oral absorption	PSA	Rule of five
Acceptable ranges	130-750	< 5	<10	2.0 – 20.0	–3.0 – 1.2	<25 Poor >500 greater	>80%is high <25% is poor	7.0-200.00	Max 4
T1	379.389	1	6.25	235.872	-1.387	187.022	87.582	116.128	0
T2	413.834	1	6.25	238.955	-1.221	451.031	90.728	115.726	0
T3	413.834	1	6.25	259.568	-1.162	419.28	90.731	116.137	0
T4	458.285	1	6.25	242.132	-1.206	491.13	91.293	115.733	0
T5	409.416	1	7	235.991	-1.473	182.53	88.5	124.443	0
T6	395.389	2	7	99.451	-1.869	72.939	77.363	135.726	0
T7	409.416	1	7	259.162	-1.429	205.782	89.274	121.51	0
T8	424.387	1	7.25	28.812	-2.517	19.132	67.155	160.963	0
T9	409.416	1	7	233.696	-1.515	183.758	88.222	124.193	0
T10	448.28	1	6.25	258.525	-1.048	858.024	93.149	115.619	0
T11	439.442	1	7.75	411.558	-1.08	290.245	96.37	125.374	0
T12	469.468	1	8.5	418.27	-1.166	294.288	92.571	136.57	0
T13	394.404	2.5	7.25	95.51	-1.869	70.566	75.749	139.144	0
T14	393.416	1	6.25	298.236	-1.282	238.972	91.296	114.986	0
T15	393.416	1	6.25	70.854	-2.015	49.277	74.36	138.703	0
T16	458.285	1	6.25	236.362	-1.229	487.908	90.958	115.735	0
T17	472.312	1	6.25	245.378	-1.326	503.338	93.49	116.134	0
T18	395.389	2	7	70.743	-2.066	50.528	74.288	138.608	0
T19	425.415	2	7.75	81.8	-2.073	59.684	75.865	143.728	0
T20	393.416	1	6.25	235.279	-1.426	182.574	89.694	116.192	0
T21	411.388	3	7.75	26.236	-2.59	17.277	62.513	160.138	0
T22	427.388	4	8.5	9.392	-3.172	5.692	50.181	181.667	0
T23	435.497	1	6.25	232.7	-1.576	182.837	94.804	116.130	0
T24	422.458	1	7.25	235.375	-1.498	175.099	90.525	119.538	0
T25	429.449	1	6.25	234.157	-1.493	184.087	93.253	115.986	0
Methotrexate (Std)	454.444	6.25	11.75	0.06	-4.671	0.022	0	233.239	2
5-fluorouracil (Std)	130.078	2	3.5	187.736	-0.673	142.642	65.585	87.585	0
Cyclophosphamide (Std)	261.087	1	8.5	3262.693	0.319	10000	94.796	40.602	0

3.2. MM-GBSA Assay

The target protein and the relevant protein were made in accordance with the structure as shown in Fig-1. All of these suggested analogues had strong free binding energies and will match the AXL receptor well. The binding free energies of the Compound T21 have the highest ΔG binding energy to 5TD2 with a value of -92.51 kcal/mol compared to the known standard drug, and Cyclophosphamide having ΔG binding energy of -49.32 kcal/mol.

3.3. ADMET studies

Many drugs fail mostly during the drug discovery process owing to toxicity, blood-brain permeation failure, and low efficacy. Because most anticancer medicines have poor pharmacokinetic qualities, were designed molecules and their properties were studied. In therapeutic development, the properties of absorption, distribution, metabolism, excretion, and toxicity (ADMET) are critical. Failures in drug discovery are mainly related to lack of efficacy and severe toxicity. The ability of medications to traverse membranes and cytosol to reach their target is dependent on their lipophilic properties. ADMET-related parameters such as water solubility, CYP450, human intestine absorption, plasma protein binding, oral bioavailability, volume of distribution, blood-brain barrier penetration, transporter, and safety are used to refine drug similarity features (Life and software package, version 3.5 2008). The ADMET characteristics of the linked 1,3,4oxadiazolederivatives were anticipated in this study using the ADMETSAR dataset, which is an open source. Several ADMET related factors, such as oral bioavailability, water solubility, human intestine absorption, blood-brain barrier penetration renal, organic cation transporter, CYP450 substrates, P-glycoprotein substrate and inhibitor, inhibition (CYP1A2, 2C9, 2C19, 2D6, and 3A4), the volume of distribution, plasma protein

binding, human Ether-ago-go-Related gene (hERG) inhibition, rat acute toxicity, drug-induced liver injury skin sensitivity, carcinogens, AMES mutagenicity, the Tetrahymenapyriformis toxicity, and fish toxicity have been predicted. The probabilities of thiazolidinedione linked 1,3,4 oxadiazole being blood-brain barrier penetration, CYP450 substrates and inhibition, human intestinal absorption, AMES mutagenicity, and human Ether-a-go-goRelated gene (hERG) inhibition, fish toxicity, carcinogenicity, Caco-2 Permeability, aqueous solubility (LogS), and rat acute toxicity range from 0.5190-0.8248. The comprehensive anticipated properties of other investigated compounds in relation to thiazolidinedione analogs are shown in (Table- 4).

Blood-brain barrier penetration probabilities of compounds T1, T2, T3, T4, T10, T16, T19, and T25 are higher than the standard. Probabilities of human intestinal absorption range from 0.9774 to 1.0000. Proposed compounds have stronger ADME characteristics and so have a higher likelihood of becoming lead compounds. In addition, pharmaceutically important features of thiazolidinedione analogs were examined using QikProp software (Table-5) and distinguished to reference medications Methotrexate, 5-fluorouracil, and Cyclophosphamide. The QikProp results revealed the discovery of compounds (T1-T25) with good ADME properties. Molecular weight (mol MW) (150–500), aqueous solubility (QPlogS) (-6.5 to 0.5), apparent MDCK cell permeability (QPPMDCK) (500 great), percent human oral absorption and brain/blood partition coefficient (QPlogBB) (-3.0 to 1.2) are the primary descriptors presented in QikProp (Schrodinger) software (C80 percent is high, B25 percent is deficient). All substances examined have an oral absorption rate of 80–100% in humans (Table-5). The first three properties, molecular weight (mol MW) less than 650, solubility (QPlogS) greater than -7, and partition coefficient between octanol and water (logPo/w) between -2 and 6.5, are based on the Lipinski rule of five. The brain/blood partition coefficient (QPlogBB) measure determines a drug's capacity to pass the blood-brain barrier, which is important in ADME druggability studies. A drug-likeness test is performed using Lipinski's rule of five pharmacokinetics filter. According to this criterion, orally administered medications must have a molecular weight (MW) of 500 or less, ten or fewer hydrogen bond acceptor sites (N and O atoms), a logP of five or less, and five or few hydrogen bonds donor sites. All compounds in this study have H donor sites of less than five and H acceptor sites of less than ten. T1-T25 is estimated to have a molecular weight of less than 500. In addition, topological polar surface area analysis was used to determine the bioavailability of all the designed analogs. Using topological PSA, the polar surface area (PSA) was estimated. This descriptor has been connected to drug bioavailability and has been correlated well with passive molecular transport through membranes. As an outcome, it can be used to predict drug transport qualities. Any molecule having a PSA value of less than 100 A° 2 is thought to be capable of sound absorption. Oral bioavailability is anticipated to be limited for passively absorbed compounds with a PSA 140 A˚ 2. All of the developed molecules have a PSA value that is within the limit (Table-5)

4. Conclusion

Thiazolidinedione has gained medicinal importance due to its various pharmacological and biological profiles, making it a unique molecule for multiple studies. Likewise, 1,3,4-oxadiazoles are well-known substances in the realm of organic chemistry. In-silico investigations were used to examine the hybrids of these moieties for potential anticancerous action. According to the investigation, the 1,3,4-oxadiazole moiety-linked thiazolidinedione exhibited outstanding binding energy and G score. The choice of the AXL receptor has shown that these hybrid compounds have a promising level of activity. To validate its enhanced SAR, the work still needs more in vitro and in vivo investigations. The developed compounds have impressively displayed anticancer activities in the in-silico investigations. The compounds T22, T21, T19, and T15 have shown strong anti-breast cancer action, and these analogues are recognized as promising molecules and still need to undergo structural modifications by the wet lab procedure in order to produce the lead molecules.

Acknowledgements

The authors express sincere thanks to NGSM Institute of Pharmaceutical Science and Nitte (Deemed to be University) Mangalore, Karnataka and NGSM-CADD Lab for providing all the necessary facilities required to carry out this research work.

References

Al-Khayyat MZ.2021. *In silico* screening for inhibitors targeting 4-diphosphocytidyl-2- c-methyl-d-erythritol kinase in *salmonella typhimurium. Jordan J Bio Sci.***14(1):** 75-82.

doi.org/10.54319/jjbs/140110

Alzhrani, Z. M. M., Alam, M. M., Neamatallah, T., and Nazreen, S. 2020.Design, synthesis and in vitro antiproliferative activity of new thiazolidinedione-1, 3, 4-oxadiazole hybrids as thymidylate synthase inhibitors. *J Enzyme Inhib Med Chem.* **35(1):** 1116-23. doi: 10.1080/14756366.2020.175958

Batra B, SudanSS, PantM, PantK, Lal A and Gusain T. 2022. Molecular docking and tlc analysis of candidate compounds from lesser used medicinal plants against diabetes mellitus targets. *Jordan J Bio Sci.***15(2):**339-346. doi.org/10.54319/jjbs/150221

Belfiore, A., Genua, M., and Malaguarnera, R. 2009. PPAR-agonists and their effects on IGF-I receptor signaling: implications for cancer. *PPAR Research*. 2009: 830501.
doi: 10.1155/2009/830501

Chen, R., Yan, J., Liu, P., and Wang, Z. 2015. Effects of thiazolidinedione therapy on inflammatory markers of type 2 diabetes: a meta-analysis of randomized controlled trials. *PloSOne*. **10(4):** e0123703.
doi: 10.1371/journal.pone.0123703.

Dey S, KaushikG, Mahanta Sand Chakraborty A.2021. Homology modeling of apoprotein Opsin and covalent docking of 11-cis retinal and 11-cis 3, 4-didehyroretinal to obtain structures of Rhodopsin and Porphyropsin from Zebra danio, *Danio rerio* (Hamilton, 1822). *Jordan J Bio Sci.***14(4):** 727-732.
doi.org/10.54319/jjbs/140413

Feneyrolles, C., Spenlinhauer, A., Guiet, L., Fauvel, B., Daydé-Cazals, B., Warnault, P., .and Yasri, A. 2014. AXL kinase as a key target for oncology: focus on small molecule inhibitors. *Mol Cancer Ther*. **13(9):** 2141-48. doi: 10.1158/1535-7163

Gay, C. M., Balaji, K., and Byers, L. A. 2017. Giving AXL the axe: targeting AXL in human malignancy. *Br J Cancer*. **116(4)**: 415-23. doi: 10.1038/bjc.2016.428

Gjerdrum, C., Tiron, C., Høiby, T., Stefansson, I., Haugen, H., Sandal, T., ...and Lorens, J. B. 2010. AXL is an essential epithelial-to-mesenchymal transition-induced regulator of breast cancer metastasis and patient survival. Proc Natl Acad Sci USA. **107(3):** 1124-29. doi: 10.1073/pnas.0909333107

He, L., Zhang, J., Jiang, L., Jin, C., Zhao, Y., Yang, G., and Jia, L. 2010. Differential expression of AXL in hepatocellular carcinoma and correlation with tumor lymphatic metastasis. *Mol Carcinog*. **49(10):** 882-91. doi.org/10.1002/mc.20664

Hu, C. F., Zhang, P. L., Sui, Y. F., Lv, J. S., Ansari, M. F., Battini, N., and Geng, R. X. 2020. Ethylenic conjugated coumarin thiazolidinediones as new efficient antimicrobial modulators against clinical methicillin-resistant Staphylococcus aureus. *Bioorg Chem.* **94:** 103434. doi: 10.1016/j.bioorg.2019.10343

Ito, T., Ito, M., Naito, S., Ohtsuru, A., Nagayama, Y., Kanematsu, T., and Sekine, I. 1999.Expression of the AXL receptor tyrosine kinase in human thyroid carcinoma. *Thyroid.* **9(6):** 563-67. doi: 10.1089/thy.1999.9.563.

Jänne, P. A., Yang, J. C. H., Kim, D. W., Planchard, D., Ohe, Y., Ramalingam, S. S., and Ranson, M. (2015). AZD9291 in EGFR inhibitor–resistant non–small-cell lung cancer. *N Engl J Med*. **372(18):** 1689-99. doi: 10.1056/NEJMoa1411817.

Knight, S. D., Adams, N. D., Burgess, J. L., Chaudhari, A. M., Darcy, M. G., Donatelli, C. A., and Dhanak, D. 2010. Discovery of GSK2126458, a highly potent inhibitor of PI3K and the mammalian target of rapamycin. *ACS Med Chem Lett*. **191(1):** 39-43. doi: 10.1021/ml900028r

Lee, W.H., and Kim, S.G. 2010.AMPK-dependent metabolic regulation by PPAR agonists. *PPAR Res.* **2010.** : 2010:549101. doi: 10.1155/2010/549101.

Liu, K., Rao, W., Parikh, H., Li, Q., Guo, T. L., Grant, S.,and Zhang, S. 2012. 3, 5-Disubstituted-thiazolidine-2, 4-dione analogs as anticancer agents: design, synthesis and biological characterization. *Eur J Med Chem***47**: 125-37. doi: 10.1016/j.ejmech.2011.10.031

Musetti, S. N., and Huang, L. 2021. Tinagl1 gene therapy suppresses growth and remodels the microenvironment of triple negative breast cancer. *Mol Pharm.* **18(5):** 2032-38. doi: 10.1021/acs.molpharmaceut.1c00008.

Narukawa, T., Hongo, F., Fujihara, A., Ueno, A., Matsugasumi, T., and Ukimura, O. 2020. Pazopanib after Nivolumab-Induced Tumor Lysis Syndrome in a Patient with Metastatic Clear-Cell Renal Cell Carcinoma. *Case Rep Oncol.* **13(1):** 249-54. doi: 10.1159/000506196

Nazreen, S., Alam, M. S., Hamid, H., Yar, M. S., Shafi, S., Dhulap, A., and Pillai, K. K. 2014. Design, synthesis, in silico molecular docking and biological evaluation of novel oxadiazole based thiazolidine-2, 4-diones bis-heterocycles as PPAR-γ agonists. *Eur J Med Chem*. **87:** 175-85. doi: 10.1016/j.ejmech.2014.09.010

Paccez, J.D., Vasques, G.J., Correa, R.G., Vasconcellos, J.F., Duncan, K., Gu, X., Bhasin, M., Libermann, T.A, and Zerbini L.F. 2013.The receptor tyrosine kinase AXL is an essential regulator of prostate cancer proliferation and tumor growth and represents a new therapeutic target. *Oncogene*.**32(6):**689-98. doi: 10.1038/onc.2012.89.

Savitri AD, Hidayati HB, Veterini L, Widyaswari MS, Muhammad AR, Fairus A, Zulfikar MQB, Astri M, Ramasima NA, Anggraeni DP, Nainatika RSA and Juliana.2023. An in-silico study on allicin compound in garlic (allium sativum) as a potential inhibitor of human epidermal growth factor receptor (her)-2 positive breast cancer. *Jordan J Bio Sci*.**16(1)**:7-12. doi.org/10.54319/jjbs/160102

Shankar, S., and Vuppu, S. 2020.In vitro drug metabolism and pharmacokinetics of a novel thiazolidinedione derivative, a potential anticancer compound. *J Pharm Biomed Anal*. **179**: 113000. doi: 10.1016/j.jpba.2019.113000

Shen, W., Xi, H., Li, C., Bian, S., Cheng, H., Cui, J.and Chen, L. 2019. Endothelin-A receptor in gastric cancer and enhanced antitumor activity of trastuzumab in combination with the endothelin-A receptor antagonist ZD4054. *Ann N Y Acad Sci.* **1448(1):** 30-41. doi: 10.1111/nyas.14053

Shimazaki, N., Togashi, N., Hanai, M., Isoyama, T., Wada, K., Fujita, T.,andKurakata, S. 2008. Anti-tumour activity of CS-7017, a selective peroxisome proliferator-activated receptor gamma agonist of thiazolidinedione class, in human tumour xenografts and a syngeneic tumour implant model. *Eur J Cancer*. **44(12):** 1734-43. doi:10.1016/j.ejca.2008.04.016

Siegel, R. L., Miller, K. D., and Jemal, A. 2016.Cancer statistics, 2016. *CA: Cancer J Clin*. **66(1):** 7-30. doi: 10.3322/caac.21332

Smallridge, R. C., Copland, J. A., Brose, M. S., Wadsworth, J. T., Houvras, Y., Menefee, M. E., and Von Roemeling, R..2013. Efatutazone, an oral PPAR-γ agonist, in combination with paclitaxel in anaplastic thyroid cancer: results of a multicenter phase 1 trial. *J Clin Endocrinol Metab*. **98(6):** 2392-2400. doi: 10.1210/jc.2013-1106.

Subbiah, V., Meyer, C., Zinner, R., Meric-Bernstam, F., Zahurak, M. L., O'Connor, A., and Azad, N. A. 2017. Phase Ib/II study of the safety and efficacy of combination therapy with multikinase VEGF inhibitor pazopanib and MEK inhibitor trametinib in advanced soft tissue sarcoma. *Clin Cancer Res.* **23(15):** 4027-34. doi: 10.1158/1078-0432.CCR-17-0272.

Tokala, R., Thatikonda, S., Sana, S., Regur, P., Godugu, C., and Shankaraiah, N. 2018. Synthesis and in vitro cytotoxicity evaluation of β-carboline-linked 2, 4-thiazolidinedione hybrids: potential DNA intercalation and apoptosis-inducing studies. *New J Chem*. **42(19):** 16226-36. https://doi.org/10.1039/C8NJ03248C

Trotsko, N., Przekora, A., Zalewska, J., Ginalska, G., Paneth, A., and Wujec, M. 2018. Synthesis and in vitro antiproliferative and antibacterial activity of new thiazolidine-2, 4-dione derivatives. *J Enzyme Inhib Med Chem*. **33(1):** 17-24. doi: 10.1080/14756366.2017.1387543

Xu, C., Han, Y., Xu, S., Wang, R., Yue, M., Tian, Y. and Gong, P. 2020. Design, synthesis and biological evaluation of new AXL kinase inhibitors containing 1, 3, 4-oxadiazole acetamide moiety as novel linker. *Eur J Med Chem*. **186:** 111867. doi: 10.1016/j.ejmech.2019.111867.